Sādhanā (2018) 43:13
https://doi.org/10.1007/s12046-017-0769-7

A two-dimensional problem of a mode-I crack in a rotating fibre-reinforced isotropic thermoelastic medium under dual-phase-lag model

AHMED E ABOUELREGAL[1] and S M ABO-DAHAB[2,3,*]

[1]Department of Mathematics, Faculty of Science, Mansoura University, P. O. Box 35516, Mansoura, Egypt
[2]Department of Mathematics, Faculty of Science, South Valley University, Qena 83523, Egypt
[3]Department of Mathematics, Faculty of Science, Taif University, Taif 888, Saudi Arabia
e-mail: ahabogal@mans.edu.eg; sdahb@yahoo.com

MS received 13 May 2014; revised 29 October 2016; accepted 9 June 2017; published online 7 February 2018

Abstract. In the present work, a general model of the equations of generalized thermoelasticity for a homogeneous isotropic elastic half-space solid whose surface is subjected to a mode-I crack problem under the effect of rotation is investigated. The normal mode analyses are used to obtain the expressions for the temperature distribution, the displacement component and thermal stresses in the context of the dual-phase-lag theory of thermoelasticity proposed by Tzou. The boundary of the crack is subjected to a prescribed stress distribution and temperature. Some particular cases are also discussed in the context of the problem. The numerical values of the temperature distribution, the displacement components and thermal stresses are also computed for a suitable material and the results are presented graphically. The effects of rotation, reinforcement and the phase lags parameters are discussed in detail in the light of earlier works.

Keywords. Fibre-reinforced; mode-I crack; dual-phase-lag theory; rotation; normal mode analysis.

1. Introduction

The theory of thermoelasticity to include the effect of temperature change has been well established. According to the theory, the temperature field is coupled with the elastic strain field. In thermoelasticity, classical heat transfer, Fourier's conduction equation is extensively used in many engineering applications. Biot [1] explained thermoelasticity by deriving dilatation based on the thermodynamics of irreversible process and coupling it with elastic deformation. However, the diffusion-type heat equation used in this study predicted infinite speed for propagation of thermal signals. The classical theory of thermoelasticity Nowacki [2, 3] rests upon the hypothesis of the Fourier law of heat conduction, in which the temperature distribution is governed by a parabolic-type partial differential equation. Consequently, the theory predicts that a thermal signal is felt instantaneously everywhere in a body. This implies that an infinite speed of propagation of the thermal signal, which is impractical from the physical point of view, particularly for short-time. Thus, the use of Fourier's equation may result in discrepancies under some special conditions, such as low-temperature heat transfer, high frequency or ultrahigh heat flux heat transfer, and so on. Lord and Shulman [4] defined a generalized theory of thermoelasticity using a hyperbolic equation of heat conduction with a relaxation time that ensured finite speed for thermal signals.

Thermoelasticity has wide applications in various fields, especially, earthquake engineering, soil dynamics, aeronautics, astronautics, nuclear reactors, high-energy particle accelerators, etc. Thermoelasticity is also used in polymer coating and to evaluate the stress redistribution in ceramic matrix composites. Thermoelasticity deals with dynamical systems whose interactions with surroundings include not only mechanical work and external work but also exchange of heat. Using two relaxation times, Green and Lindsay [5] developed another generalized theory of thermoelasticity. These works include the time needed for the acceleration of heat flow and take into account the coupling between temperature and strain fields for isotropic materials. The theory of thermoelasticity without energy dissipation is another generalized theory and was formulated by Green and Naghdi [6]. It includes the "thermal displacement gradient" among its independent constitutive variables, and differs from the previous theories in that it does not accommodate dissipation of thermal energy Ignaczak and Ostoja-Starzewski [7].

Tzou [8–10] proposed the dual-phase-lag (DPL) model, which describes the interactions between phonons and electrons at the microscopic level as retarding sources

*For correspondence

causing a delayed response on the macroscopic scale. For macroscopic formulation, it would be convenient to use the DPL mode for investigation of the micro-structural effect on the behaviour of heat transfer. The physical meanings and the applicability of the DPL mode have been supported by the experimental results Tzou [10]. The DPL mode can be developed to the hyperbolic two-step model, the parabolic two-step model, Jeffreys-type heat flux model, microscopic phonon-scattering model, the thermal wave model and the classical diffusion model. It covers a wide scale of space and time for physical observations. Some heat transfer problems in layered media have been analysed with the DPL mode.

Materials such as resins reinforced by strongly aligned fibres exhibit highly anisotropic elastic behaviour in the sense that their elastic moduli for extension in the fibre direction are frequently on the order of 50 or more times greater than their elastic moduli in transverse extension or in shear. The mechanical behaviour of many fibre-reinforced composite materials is adequately modelled by the theory of linear elasticity for transversely isotropic materials, with the preferred direction coinciding with the fibre direction. In such composites the fibres are usually arranged in parallel straight lines. However, other configurations are also used. An example is that of circumferential reinforcement, for which the fibres are arranged in concentric circles, giving strength and stiffness in the tangential (or hoop) direction. The analysis of stress and deformation of fibre-reinforced composite materials has been an important subject of solid mechanics for the last three decades. The characteristic property of a reinforced concrete member is that its components, namely concrete and steel, act together as a single anisotropic unit as long as they remain in the elastic condition, i.e., the two components are bound together so that there can be no relative displacement between them.

The idea of introducing a continuous self-reinforcement at every point of an elastic solid was given by Belfied *et al* [11]. The model was later applied to the rotation of a tube by Verma and Rana [12]. Sengupta and Nath [13] discussed the problem of the surface waves in fibre-reinforced anisotropic elastic media. Hashin and Rosen [14] gave the elastic moduli for fibre-reinforced materials. The problem of reflection of plane waves at the free surface of a fibre-reinforced elastic half-space was discussed by Singh and Singh [15]. Singh [16] discussed the wave propagation in an incompressible transversely isotropic fibre-reinforced elastic medium. Singh [17] studied the effects of anisotropy on reflection coefficients of plane waves in a fibre-reinforced thermoelastic solid. Kumar and Gupta [18] investigated a source problem in fibre-reinforced anisotropic generalized thermoelastic solid under acoustic fluid layer. Ailawalia and Budhiraja [19] discussed the effect of hydrostatic initial stress on fibre-reinforced generalized thermoelastic medium. Abbas and Abd-Alla [20] studied the effect of initial stress on a fibre-reinforced anisotropic thermoelastic thick plate. Allam *et al* [21] applied the Green and Naghdi (GN) theory on electromagneto-thermoelastic problem to a thick plate. Cheng and Zhang [22] investigated the normal mode expansion method for laser-generated ultrasonic Lamb waves in orthotropic thin plates.

It appears that little attention has been paid to study the propagation of plane thermoelastic waves in a rotating medium. Since most large bodies like the earth, the moon and other planets have an angular velocity, it appears more realistic to study the propagation of plane thermoelastic or magneto-thermoelastic waves in a rotating medium with phase lags. Paria [23] and Wilson [24] investigated the propagation of magneto-thermoelastic waves in a nonrotating medium. These studies, based on the theory of classical coupled thermoelasticity (CTE), were essentially concerned with the interaction of the electromagnetic field, the thermal field and the elastic field, as well as the dispersion relation. In a paper by Schoenberg and Censor [25], the propagation of plane harmonic waves in a rotating elastic medium has been investigated in some detail. It has been shown that the rotation causes the elastic medium to be dispersive and anisotropic. This study included some discussion on the free-surface phenomenon in a rotating half-space. Results concerning slowness surfaces, energy flux, reflected waves and generalized Rayleigh waves have been obtained. Later on, several authors Puri [26], Roychoudhury and Debnath [27], Roychoudhury [28], Chandrasekharaiah and Srikantian [29], Chandrasekharaiah [30] studied plane waves in rotating thermoelastic and magneto-thermoelastic media in the context of generalized theories. It seems relevant from this discussion that little attention has been given to the study of propagation of thermoelastic plane waves in a rotating medium in the presence of an external magnetic field based on the generalized thermoelasticity. In view of the fact that most large bodies like the earth, the moon and other planets have an angular velocity, it is important to consider the propagation of magneto-thermoelastic plane waves in an electrically conducting, rotating, viscoelastic medium under the action of an external magnetic field. Abo-Dahab [31] investigated the influence of magneto-thermo-viscoelasticity in an unbounded body with a spherical cavity subjected to harmonically varying temperature without energy dissipation. Recently, Abouelregal and Abo-Dahab [32] investigated DPL model on magneto-thermoelastic infinite nonhomogeneous solid having a spherical cavity. Mahmoud [33] studied the problem of shear waves in magneto-elastic half-space of initially stressed non-homogeneous anisotropic material under the influence of rotation. Some new recently works related to the present estimation have been discussed [34–44].

The aim of this paper is to determine the normal displacement, normal force stress and temperature distribution in a fibre-reinforced generalized thermoelastic medium that is rotating with a uniform angular velocity by the DPL theory of thermoelasticity. The normal mode analysis is used to obtain exact expressions for the displacement components, force stresses and temperature. The variations of the considered variables with the horizontal distance are illustrated graphically. Comparisons are made with the results in the

presence and absence of fibre reinforcement and rotation. The results reduce to corresponding classical results when the reinforcement elastic parameters tend to zero and the medium becomes isotropic. The effects of phase lags, reinforcement and rotation on the variations of different field quantities inside the medium are analysed graphically. It has been found that the different field quantities are affected both by rotation as well as by the phase lags.

2. Basic equations

We consider an infinite isotropic, homogeneous, thermally conducting elastic medium with density ρ at uniform initial temperature T_0. The medium rotates at an angular velocity $\mathbf{\Omega} = \Omega\mathbf{n}$, where $\mathbf{n}$ is a unit vector representing the direction of the axis of rotation. The displacement equation of motion in rotating frame of reference has two additional terms: centripetal acceleration $\mathbf{\Omega} \times (\mathbf{\Omega} \times \mathbf{u})$ due to the time-varying motion only and the Coriolis acceleration $2(\mathbf{\Omega} \times \dot{\mathbf{u}})$, where $\mathbf{u}$ is the dynamic displacement vector Schoenberg and Censor [25]. These terms do not appear in a nonrotating medium. The dynamic displacement vector is actually measured from a steady-state deformed position and the deformation is assumed to be small.

The principle of balance of linear momentum leads to the following equations of motion:

$$\sigma_{ji,j} = \rho\left[\left(\frac{\partial^2 \mathbf{u}}{\partial t^2}\right)_i + (\mathbf{\Omega} \times (\mathbf{\Omega} \times \mathbf{u}))_i + 2(\mathbf{\Omega} \times \dot{\mathbf{u}})_i\right] \tag{1}$$

where σ_{ji} are the components of stress, u_i are the components of displacement vector, $i,j = 1,2,3$ refer to general coordinates and $\mathbf{\Omega} = (0,0,\Omega)$.

The Tzou theory is a modified classical thermoelasticity model in which the Fourier law is replaced by the approximation equation

$$q(x, t + \tau_q) = -K\nabla(x, t + \tau_\theta).$$

Thermoelastic disturbances transmitted in a wave-like manner are approximated in the form

$$\left(1 + \tau_q \frac{\partial}{\partial t}\right) q_i = -K\left(1 + \tau_\theta \frac{\partial}{\partial t}\right)\nabla T.$$

Hence, we get the heat conduction equation in the context of DPL model containing the thermoelastic coupling term in the following form Tzou [10]:

$$K\left(1 + \tau_\theta \frac{\partial}{\partial t}\right)\nabla^2 T = \left(\delta + \tau_q \frac{\partial}{\partial t}\right)\left(\rho C_E \frac{\partial T}{\partial t} + \gamma T_0 \frac{\partial e}{\partial t}\right) \tag{2}$$

where K is the thermal conductivity, t_0 is a constant with the dimension of time that acts as a relaxation time, C_E is the specific heat at constant strain, T_0 is the temperature of the medium in its natural state, assumed to be such as $|(T - T_0)/T| \ll 1$, $\gamma = (3\lambda + 2\mu)\alpha_t$ and α_t is the thermal expansion coefficient, τ_θ is the phase lag of the heat flux, τ_q is phase lag of gradient of temperature and $0 \le \tau_\theta < \tau_q$, and e_{ij} are the components of the strain tensor.

The constitutive equations for a fibre-reinforced linearly elastic anisotropic medium with respect to the reinforcement direction $\mathbf{b} \equiv (b_1, b_2, b_3)$ with $b_1^2 + b_2^2 + b_3^2 = 1$ are

$$\begin{aligned}\sigma_{ij} = {} & \lambda e_{kk}\delta_{ij} + 2\mu_T e_{ij} + \alpha\left(b_k b_m e_{km}\delta_{ij} + b_i b_j e_{kk}\right) \\ & + 2(\mu_L - \mu_T)\left(b_k b_i e_{kj} + b_k b_j e_{ki}\right) \\ & + \beta b_k b_m e_{km} b_i b_j - \gamma(T - T_0)\end{aligned} \tag{3}$$

where e_{ij} are the components of strain, λ, μ_T are the elastic constants and α, β, $(\mu_L - \mu_T)$ are the reinforcement parameters. The comma notation is used for spatial derivatives and superimposed dot represents time differentiation. The strain–displacement relation is

$$e_{ij} = \frac{1}{2}\left(u_{i,j} + u_{j,i}\right).$$

3. Problem formulation

In the present paper, we consider a problem of a fibre-reinforced anisotropic half-space $(x \ge 0)$. All the considered functions will depend on the time t and the coordinates (x, y, z). For the two-dimensional problem, we assume the components of the displacement vector of the form

$$u = u_1 = u(x,y,t), \qquad v = u_2 = v(x,y,t), \qquad w = u_3 = 0,$$

and assume that the solutions are independent of z, i.e., $\partial/\partial z = 0$.

We choose the fibre-direction as $\mathbf{b} = (1,0,0)$, so that the preferred direction is the x axis. Equation (3) then yields

$$\begin{aligned}\sigma_{xx} = {} & (2(\alpha + \mu_T) + 4(\mu_L - \mu_T) + \beta)\frac{\partial u}{\partial x} \\ & + (\alpha + \lambda)\frac{\partial v}{\partial y} - \gamma(T - T_0),\end{aligned} \tag{4}$$

$$\sigma_{yy} = (\alpha + \lambda)\frac{\partial u}{\partial x} + (\lambda + 2\mu_T)\frac{\partial v}{\partial y} - \gamma(T - T_0), \tag{5}$$

$$\sigma_{zz} = (\alpha + \lambda)\frac{\partial u}{\partial x} + \lambda\frac{\partial v}{\partial y} - \gamma(T - T_0), \tag{6}$$

$$\sigma_{yy} = \mu_L\left(\frac{\partial u}{\partial y} + \frac{\partial v}{\partial x}\right), \qquad \sigma_{xz} = \sigma_{yz} = 0. \tag{7}$$

Using the summation convection, from Eqs. (4)–(7), the equations of motion (1) become

$$A_{11}\frac{\partial^2 u}{\partial x^2}+B_1\frac{\partial^2 u}{\partial y^2}+B_2\frac{\partial^2 v}{\partial x\partial y}-\beta_1\frac{\partial T}{\partial x}=\rho\left(\frac{\partial^2 u}{\partial t^2}-\Omega^2 u-2\Omega\dot{v}\right), \tag{8}$$

$$A_{22}\frac{\partial^2 v}{\partial y^2}+B_1\frac{\partial^2 u}{\partial x^2}+B_2\frac{\partial^2 u}{\partial x\partial y}-\beta_2\frac{\partial T}{\partial y}=\rho\left(\frac{\partial^2 v}{\partial t^2}-\Omega^2 v+2\Omega\dot{u}\right), \tag{9}$$

where

$$A_{11}=2(\alpha+\mu_T)+4(\mu_L-\mu_T)+\beta,\quad A_{12}=\alpha+\lambda,$$
$$A_{22}=\lambda+2\mu_T,\quad B_1=\mu_L,\quad B_2=\alpha+\lambda+\mu_L.$$

For convenience, the following non-dimensional variables are used:

$$x'=c_0\eta x,\quad y'=c_0\eta y,\quad u'=c_0\eta u,\quad v'=c_0\eta v,$$
$$\theta=\frac{\gamma(T-T_0)}{\lambda+2\mu_T},\quad \tau'=c_0^2\eta\tau,\quad \tau'_{q,\theta}=c_0^2\eta\tau_{q,\theta},\quad \sigma_{ij}=\frac{\sigma_{ij}}{\gamma T_0},$$
$$\Omega'=\frac{\Omega}{c_0^2\eta},\quad c_0^2=\frac{\lambda+2\mu_T}{\rho},\quad \eta=\frac{\rho C_E}{K}. \tag{10}$$

In terms of non-dimensional quantities defined in Eq. (10), the governing equations reduce to (dropping the superscript prime)

$$m_1\frac{\partial^2 u}{\partial x^2}+n_1\frac{\partial^2 u}{\partial y^2}+n_2\frac{\partial^2 v}{\partial x\partial y}-\frac{\partial T}{\partial x}=\frac{\partial^2 u}{\partial t^2}-\Omega^2 u-2\Omega\dot{v}, \tag{11}$$

$$m_2\frac{\partial^2 v}{\partial y^2}+n_1\frac{\partial^2 v}{\partial x^2}+n_2\frac{\partial^2 u}{\partial x\partial y}-\frac{\partial T}{\partial y}=\frac{\partial^2 v}{\partial t^2}-\Omega^2 v+2\Omega\dot{u}, \tag{12}$$

$$\left(1+\tau_\theta\frac{\partial}{\partial t}\right)\left(\frac{\partial^2\theta}{\partial x^2}+\frac{\partial^2\theta}{\partial y^2}\right)=\left(\delta+\tau_q\frac{\partial}{\partial t}\right)\frac{\partial\theta}{\partial t}+\varepsilon\frac{\partial}{\partial t}\left(\delta+\tau_q\frac{\partial}{\partial t}\right)\left(\frac{\partial u}{\partial x}+\frac{\partial v}{\partial y}\right), \tag{13}$$

$$\sigma_{xx}=\frac{1}{\mu_T}\left(A_{11}\frac{\partial u}{\partial x}+A_{12}\frac{\partial v}{\partial y}-A_{22}\theta\right), \tag{14}$$

$$\sigma_{yy}=\frac{1}{\mu_T}\left(A_{12}\frac{\partial u}{\partial x}+A_{22}\frac{\partial v}{\partial y}-A_{22}\theta\right), \tag{15}$$

$$\sigma_{zz}=\frac{1}{\mu_T}\left(A_{12}\frac{\partial u}{\partial x}+\lambda\frac{\partial v}{\partial y}-A_{22}\theta\right), \tag{16}$$

$$\sigma_{xy}=\frac{\mu_L}{\mu_T}\left(\frac{\partial u}{\partial y}+\frac{\partial v}{\partial x}\right) \tag{17}$$

where

$$m_1=\frac{A_{11}}{\lambda+2\mu_T},\quad m_2=\frac{A_{22}}{\lambda+2\mu_T},\quad n_1=\frac{B_1}{\lambda+2\mu_T},$$
$$n_2=\frac{B_2}{\lambda+2\mu_T},\qquad \varepsilon=\frac{\gamma^2 T_0}{\rho C_E(\lambda+2\mu_T)}.$$

4. Normal mode analysis

The normal mode analysis gives exact solutions without any assumed restrictions on temperature, displacement and stress distributions. It is applied for a wide range of problems in different branches. It can be applied to boundary-layer problems, which are described by the linearized Navier–Stokes equations in electro hydrodynamics. The normal mode expansion method has been proposed by Cheng and Zhang [22] for modelling the thermoelastic generation process of elastic waveforms in an isotropic plate. Allam *et al* [21] used the normal mode analysis to study the two-dimensional problem of electromagneto-thermoelasticity for a homogeneous isotropic perfectly conducting thick plate subjected to a time-dependent heat source in the context of GN theory of thermoelasticity.

The solution of the considered physical variable can be decomposed in terms of normal modes and are given in the following form:

$$\left[u,v,\theta,\sigma_{ij}\right](x,y,t)=\left[u^*,v^*,\theta^*,\sigma^*_{ij}\right](x)e^{(\omega t+iay)} \tag{18}$$

where ω is the (complex) frequency, $i=\sqrt{-1}$, a is the wave number in the y-direction, and $u^*(x)$, $v^*(x)$, $\theta^*(x)$ and $\sigma^*_{ij}(x)$ are the amplitudes of the field quantities.

The normal mode analysis, in fact, comprises seeking the solution in the Fourier transformed domain, assuming that all the field quantities are sufficiently smooth on the real line such that normal mode analysis of these functions exists.

Using (18), Eqs. (11)–(17) take the forms

$$\left[m_1D^2-A_1\right]u^*+(ian_2+2\Omega\omega)Dv^*=D\theta^*, \tag{19}$$

$$\left[n_1D^2-A_2\right]v^*+(iah_2-2\Omega\omega)Du^*=ia\theta^*, \tag{20}$$

$$\left[D^2-A_3\right]\theta^*=A_4(Du^*+iav^*), \tag{21}$$

$$\mu_T\sigma^*_{xx}=A_{11}Du^*+iaA_{12}v^*-A_{22}\theta^*, \tag{22}$$

$$\mu_T\sigma^*_{yy}=A_{12}Du^*+iaA_{22}v^*-A_{22}\theta^*, \tag{23}$$

$$\mu_T\sigma^*_{zz}=A_{12}Du^*+ia\lambda v^*-A_{22}\theta^*, \tag{24}$$

$$\mu_T\sigma^*_{xy}=\mu_L(iau^*+Dv^*) \tag{25}$$

where

$$A_1 = \left(\omega^2 - \Omega^2 + a^2 n_1\right), \quad A_2 = \left(\omega^2 - \Omega^2 + a^2 m_2\right),$$
$$A_3 = \left(a^2 + \frac{\omega\left(\delta + \tau_q\omega\right)}{\left(1 + \tau_\theta\omega\right)}\right), \quad A_4 = \frac{\varepsilon\omega\left(\delta + \tau_q\omega\right)}{\left(1 + \tau_\theta\omega\right)}.$$

Eliminating $\theta^*(x)$ and $v^*(x)$ in Eqs. (19)–(21), we get the following sixth-order differential equation for $u^*(x)$:

$$(D^6 - AD^4 + BD^2 - C)u^*(x) = 0 \tag{26}$$

where

$$A = \frac{A_2}{n_1} + \frac{A_1 + A_4}{m_1} - \frac{n_2^2 a^2}{n_1 m_1} + A_3,$$
$$B = \frac{A_2 A_1 + A_3\left(m_1 A_2 + n_1 A_1 - n_2^2 a^2\right)}{n_1 m_1} + \frac{A_4(m_1 a^2 + A_2 - 2n_2 a^2) + 4\Omega^2\omega^2}{n_1 m_1},$$
$$C = \frac{A_1 A_3 A_2 + A_4 A_1 a^2 + 4\Omega^2\omega^2 A_3}{n_1 m_1}.$$

Introducing k_i $(i = 1, 2, 3)$ into Eq. (26), we find

$$\left(\nabla^2 - k_1^2\right)(\nabla^2 - k_2^2)(\nabla^2 - k_3^2)u^*(x) = 0 \tag{27}$$

where k_1^2, k_2^2 and k_2^2 are the roots of the characteristic equation

$$k^6 - Ak^4 + Bk^2 + C = 0. \tag{28}$$

These roots are given by

$$k_1^2 = \frac{1}{3}[2s\sin(q) + A],$$
$$k_2^2 = -\frac{s}{3}\sqrt{3}\cos(q) + \sin(q)] + \frac{A}{3},$$
$$k_3^2 = \frac{s}{3}\sqrt{3}\cos(q) - \sin(q)] + \frac{A}{3},$$
$$s = \sqrt{A^2 - 3B}, \quad q = \frac{1}{3}\sin^{-1}(R), \quad R = -\frac{2A^3 - 9AB + 27C}{2s^3}.$$

The series solution of Eq. (27), which is bounded at $x \to \infty$, is given by

$$u^*(x) = \sum_{n=1}^{3} M_n(a, \omega)e^{-k_n x}. \tag{29}$$

In a similar manner, we get

$$(D^6 - AD^4 + BD^2 - C)(v(x), \theta^*(x)) = 0. \tag{30}$$

Similarly

$$v^*(x) = \sum_{n=1}^{3} M_n'(a, \omega)e^{-k_n x}, \tag{31}$$

$$\theta^*(x) = \sum_{n=1}^{3} M_n''(a, \omega)e^{-k_n x}, \tag{32}$$

where $M_n(a, \omega)$, $M_n'(a, \omega)$ and $M_n''(a, \omega)$ are specific functions depending on a and ω. Substituting Eqs. (29)–(32) into Eqs. (19)–(21), we obtain the following relation:

$$M_n'(a, \omega) = H_{1n}M_n(a, \omega),$$
$$M_n''(a, \omega) = H_{2n}M_n(a, \omega), \quad n = 1, 2, 3$$

where

$$H_{1n} = \frac{ia(n_2 - m_1)k_n^2 + iaA_1 + 2\Omega\omega k_n}{n_1 k_n^3 + (n_2 a^2 - A_2)k_n + 2ia\Omega\omega},$$
$$H_{2n} = \frac{A_4(-k_n + iaH_{1n})}{k_n^2 - A_3}.$$

Thus, we have

$$v^*(x) = \sum_{n=1}^{3} H_{1n}M_n(a, \omega)e^{-k_n x}, \tag{33}$$

$$\theta^*(x) = \sum_{n=1}^{3} H_{2n}M_n(a, \omega)e^{-k_n x}. \tag{34}$$

Substituting Eqs. (29), (33) and (34) into Eqs. (22)–(25), we get

$$\sigma_{xx}^*(x) = \sum_{n=1}^{3} H_{3n}M_n(a, \omega)e^{-k_n x}, \tag{35}$$

$$\sigma_{yy}^*(x) = \sum_{n=1}^{3} H_{4n}M_n(a, \omega)e^{-k_n x}, \tag{36}$$

$$\sigma_{zz}^*(x) = \sum_{n=1}^{3} H_{5n}M_n(a, \omega)e^{-k_n x}, \tag{37}$$

$$\sigma_{xy}^*(x) = \sum_{n=1}^{3} H_{6n}M_n(a, \omega)e^{-k_n x} \tag{38}$$

where

$$\mu_T H_{3n} = -A_{11}k_n + iaA_{12}H_{1n} - A_{22}H_{2n},$$
$$\mu_T H_{4n} = -A_{12}k_n + iaA_{22}H_{1n} - A_{22}H_{2n},$$
$$\mu_T H_{5n} = -A_{12}k_n + ia\lambda H_{1n} - A_{22}H_{2n},$$
$$\mu_T H_{6n} = \mu_L(ia - k_n H_{1n}).$$

5. Applications

In this section, we determine the parameters $M_j(j = 1, 2, 3)$. In the physical problem, we should suppress the positive exponentials that are unbounded at infinity.

The plane boundary is subjected to an instantaneous normal point force, and the boundary surface is isothermal; the boundary conditions at the vertical plan $y = 0$ and the beginning of the crack at $x = 0$ are

$$\sigma_{yy}(x, y, t) = -P, \tag{39}$$

$$\theta(x, y, t) = F\ , \tag{40}$$

$$\sigma_{xy}(x, y, t) = 0, \tag{41}$$

$$\frac{\partial\theta(x, y, t)}{\partial y} = 0, \tag{42}$$

where P and F are the magnitudes of mechanical force and thermal source, respectively.

Substituting the expressions of the variables considered into these boundary conditions yields readily the following equations satisfied by the parameters:

$$\sum_{n=1}^{3} H_{3n} M_n(a, \omega) = -P, \tag{43}$$

$$\sum_{n=1}^{3} H_{2n} M_n(a, \omega) = F, \tag{44}$$

$$\sum_{n=1}^{3} H_{6n} M_n(a, \omega) = 0. \tag{45}$$

The resulting problem amounts to a system of three equations in the form

$$\begin{pmatrix} M_1 \\ M_2 \\ M_3 \end{pmatrix} = \begin{pmatrix} H_{41} & H_{42} & H_{43} \\ H_{21} & H_{22} & H_{23} \\ H_{61} & H_{62} & H_{63} \end{pmatrix}^{-1} \begin{pmatrix} -P^* \\ F^* \\ 0 \end{pmatrix}. \tag{46}$$

After applying the inverse of matrix method, we have the values of the three constants $M_j (j = 1, 2, 3)$. Hence, we obtain the expressions for the displacements, the temperature distribution and other physical quantities of the medium.

6. Particular and special cases

A number of special cases are pertinent to be documented here.

6.1 *Equation of CTE with reinforcement and rotation*

The equations of CTE theory are obtained when $\tau_\theta = \tau_q = 0$ and $\delta = 1$.

6.2 *Lord–Shulman with reinforcement and rotation*

The equations of the Lord–Shulman (LS) theory are retrieved when $\tau_\theta \to 0$, $\delta = 1$ and $\tau_q = t_0 > 0$.

6.3 *Equations of generalized thermoelasticity without energy dissipation with reinforcement and rotation*

The equations of the generalized thermoelasticity without energy dissipation (the linearized GN theory of type II) are obtained when $\tau_\theta \to 0$, $\delta = 0$ and $\tau_q = 1$. Also, all the results reduce to the classical isotropic results when the anisotropic parameters for the fibre-reinforced medium tend to zero (if necessary writing $\alpha = 0, \beta = 0$ and considering $|\mu_L - \mu_T| \to 0$).

Neglecting the angular velocity (i.e., $\Omega = 0$), we obtain the transformed components of displacement, stress forces and temperature distribution in a nonrotating generalized thermoelasticity medium.

7. Numerical results

In order to illustrate the theoretical results obtained in the preceding section and to compare various theories of thermoelasticity formulated earlier, we present some numerical results for the physical constants. The results depict the variations of normal displacement, normal force stress and temperature distribution in the context of fractional order thermoelasticity theory. To study the effect of reinforcement on wave propagation, we use the following physical constants for generalized fibre-reinforced thermoelastic materials Lotfy [45]:

$$\begin{aligned}
&\lambda = 7.59 \times 10^9\ \mathrm{N/m^2}, && \mu_{\mathrm{T}} = 1.89 \times 10^9\ \mathrm{N/m^2},\\
&\mu_L = 2.45 \times 10^9\ \mathrm{N/m^2}, && \alpha = -1.28 \times 10^9\ \mathrm{N/m^2},\\
&\beta = 0.32 \times 10^9\ \mathrm{N/m^2}, && \rho = 7800\ \mathrm{kg/m^3},\\
&\alpha_t = 1.78 \times 10^{-5}\ \mathrm{K^{-1}}, && \mathrm{C_E} = 383.1\ \mathrm{J/(kgK)},\\
&\tau_0 = 0.02, \quad a = 1, && T_0 = 293\ \mathrm{K}, \quad F^* = 1,\\
&P^* = 2, \quad \omega = \omega_0 + i\xi, && \omega_0 = 2, \quad \xi = 1,\\
&K = 386\ \mathrm{K/(mK)}, && \mu = 3.86 \times 10^{10}\ \mathrm{kg/ms^2}.
\end{aligned}$$

The numerical technique outlined here is used for the distribution of the real part of the temperature θ, the displacements u and v and the distributions of stresses σ_{xx}, σ_{yy} and σ_{xy} for the problem. The field quantities including temperature, displacement components u and v and stress components σ_{xx}, σ_{yy} and σ_{xy} depend not only on space x and time t but also on phase lags τ_θ and τ_q. Here all the variables are taken in the non-dimensional forms.

Tzou called the delay time τ_θ as the phase lag of the temperature gradient and the other delay time, τ_q , the phase lag of the heat flux. The delay time τ_θ is caused by the microstructural interactions (small-scale effects of heat transport in space such as phonon–electron interaction or phonon scattering). The second delay time τ_q is caused due to the fast-transient effects of thermal inertia (or small-scale effects of heat transport in time). The phase lags τ_q and τ_θ are small, positive and assumed to be intrinsic properties of the medium. We assume that the material parameters satisfy the inequality $\tau_q \geq \tau_\theta > 0$. The fundamental difference between the hyperbolic and DPL-based heat conduction equations is the extra phase lag time τ_θ. This time lag introduces an additional mechanism of diffusion in the dissipation effect in the governing equation. It is known that the lag time τ_q can dominate the behaviour of thermal wave propagation, slow down the propagation velocity of thermal signal and manifest the feature of a thermal wave. The effect of τ_θ can assist heat energy diffusion and make the characters of thermal wave decay in DPL heat transfer.

Figures 2–7 are drawn to compare the results obtained for displacements, temperature and stresses against the thickness x for different values of τ_q and τ_θ at $y = 1$. The graphs in figures 1–6 represent six curves predicted by three different theories of thermoelasticity obtained as a special case of the DPL model. The computations were performed for one value of time, namely for $t = 0.15$, and various values of the parameters τ_q and τ_θ. These computations were carried out in the coupled theory (CTE) by setting $(\tau_q = \tau_\theta = 0,\ \delta = 1)$, in LS theory (**LS**) putting $(\tau_\theta = 0,\ \tau_q > 0\ ,\ \delta = 1)$, in GN theory setting $(\tau_\theta = 0,\ \tau_q > 0,\ \delta = 1)$ and in the generalized theory of thermoelasticity proposed by Tzou (DPL) for $\tau_q \geq \tau_\theta > 0$.

Figure 2 shows the variation of temperature with x, which indicates that temperature field has the maximum value at the boundary and then decreases to zero; $y = 0$ represents the plane of the crack, which is symmetric with respect to the y plane. It is clear from the graph that θ obtains the maximum value at the beginning of the crack, and it begins to fall just near the crack edge, where it experiences smooth decreases (with the maximum negative

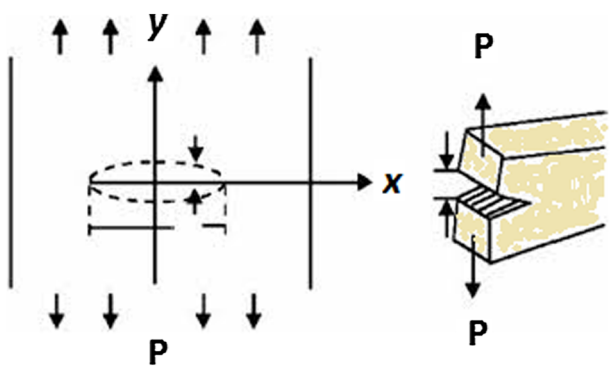

Figure 1. Schematic of the problem.

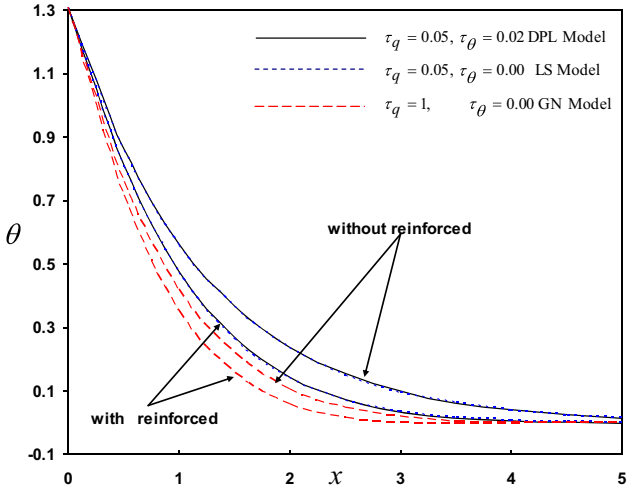

Figure 2. Dependence of temperature θ on distance for different values of phase lags in the absence and presence of fiber-reinforcement.

gradient at the crack end). The value of temperature converges to zero with the increase of distance x.

As shown in figure 3, in the case of reinforcement, horizontal displacement u increases near the crack edge, then smoothly decreases again to reach its minimum magnitude just at about the crack end and conversely in the case without reinforcement. Beyond the end, u falls again to reach zero at infinity. The values of u for GN model are larger compared with those for other theories.

Figure 4 shows vertical displacement v. We can see that, at the crack end, it reaches the maximum value. Also, it appears that the displacement component v tends to zero at the three double of the crack size (state of particle equilibrium). Displacements u and v show different behaviours,

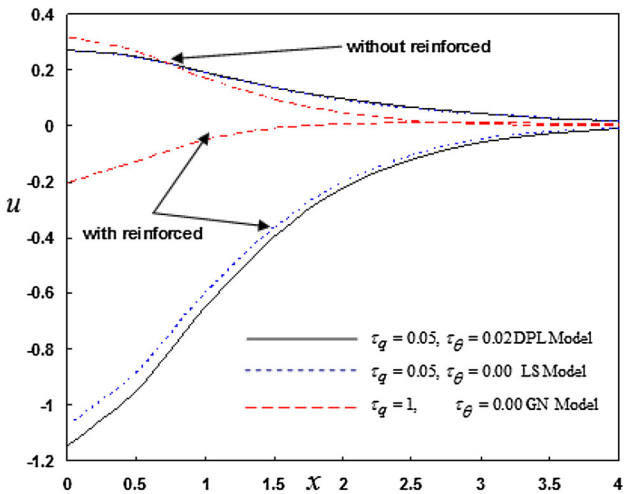

Figure 3. Dependence of horizontal displacement distribution u on distance for different values of phase lags in the absence and presence of fiber-reinforcement.

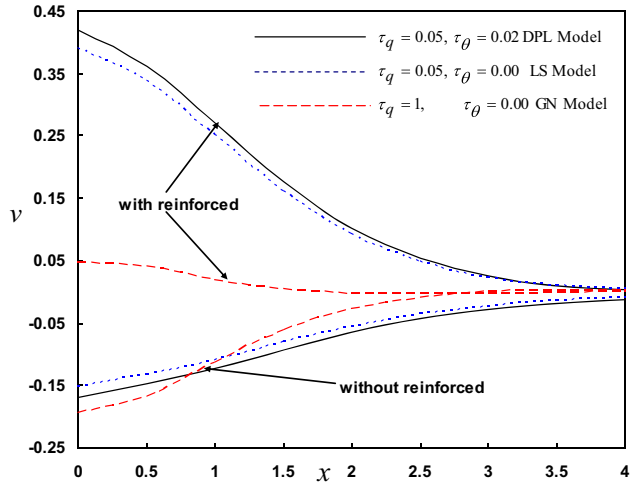

Figure 4. Dependence of vertical displacement v on distance for different values of phase lags in the absence and presence of fiber-reinforcement.

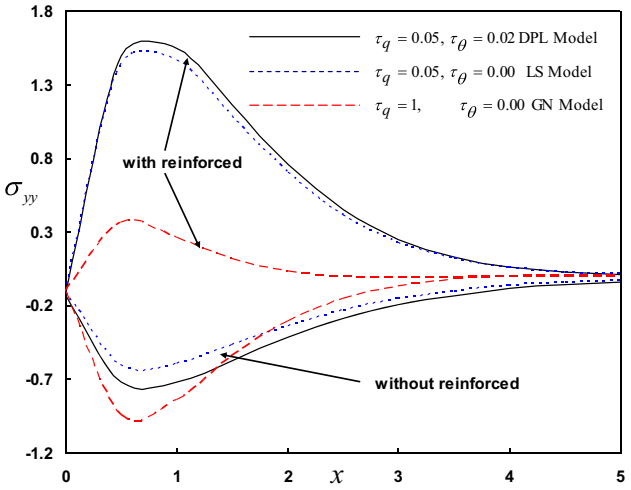

Figure 6. Dependence of stress σ_{yy} on distance for different values of phase lags in the absence and presence of fiber-reinforcement.

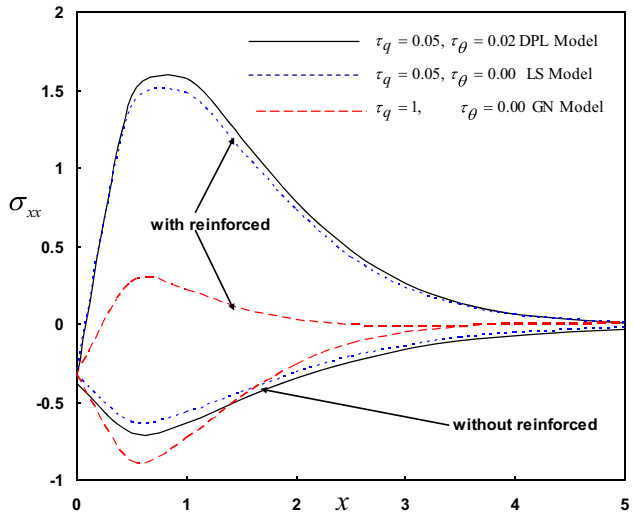

Figure 5. Dependence of stress σ_{xx} on distance for different values of phase lags in the absence and presence of fiber-reinforcement.

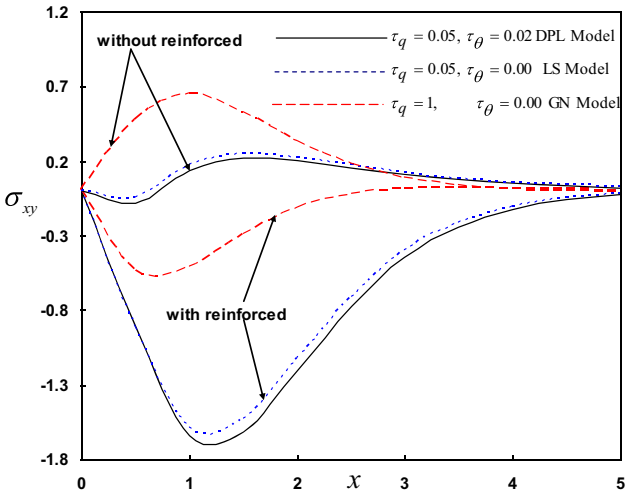

Figure 7. Dependence of stress σ_{xy} on distance for different values of phase lags in the absence and presence of fiber-reinforcement.

because the elasticity of the solid tends to resist vertical displacements in the problem under investigation. Both of the components show different behaviours. The former tends to increase to the maximum just before the end of the crack. Then it falls to the minimum with a highly negative gradient. Afterwards, it rises again to the maximum beyond the crack end.

The stress component σ_{xx} reaches coincidence with a negative value (figure 5). It reaches the minimum value near the end of the crack and converges to zero with increasing distance x. Figures 5 and 6 show the same behaviour as that found in figure 6.

Figure 7 shows that stress component σ_{xy} satisfies the boundary condition at $x = 0$ and has a different behaviour compared with that of σ_{xx}. These trends obey elastic and thermoelastic properties of the solid under investigation.

The distribution in LS theory is close to that in DPL theory, whereas the distributions in the GN theory are different from those in DPL theory. The temperature distribution decays along the direction of the transmitted wave propagation due to the effects of diffusion. By the values of τ_q and τ_θ it can be judged whether the wavelike behaviour in the DPL heat conduction is dominant or not. However, it can be found from the numerical results that the shift times τ_q and τ_θ may play a more important role in this task.

Figures 2–7 show the variation of the physical quantities with space x at $t = 0.15$ for two cases: with reinforcement

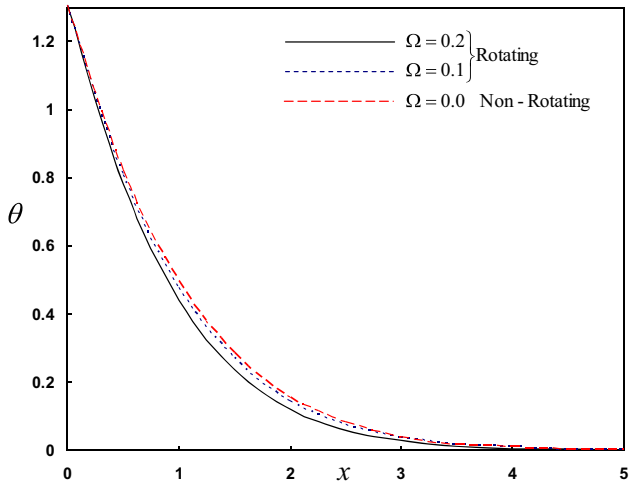

Figure 8. The temperature distribution in the case of material with phase lags in the absence and presence of fiber-reinforcement.

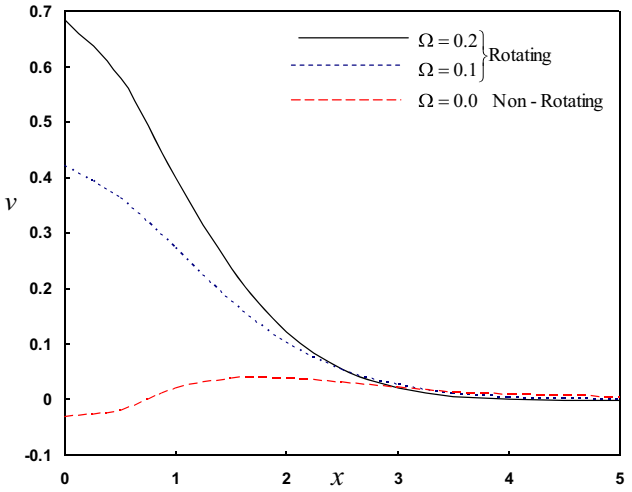

Figure 10. The displacement v distribution in the case of material with phase lags in the absence and presence of rotating.

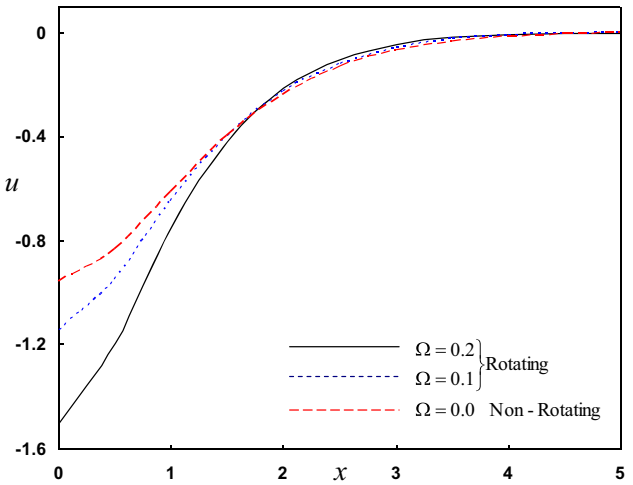

Figure 9. The displacement u distribution in the case of material with phase lags in the absence and presence of rotating.

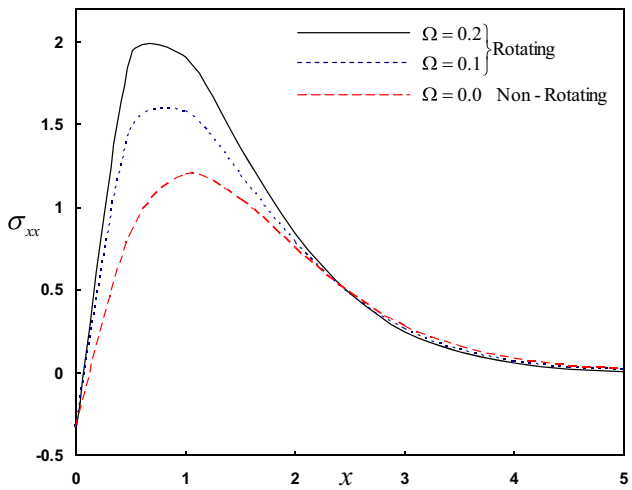

Figure 11. The stress σ_{xx} distribution in the case of material with f phase lags in the absence and presence of rotating.

and without reinforcement (i.e., $\alpha = 0$, $\beta = 0$ and $\mu_L - \mu_T = 0$). The values of v, θ and σ_{xy} are evidently smaller with reinforcement when compared with those in the absence of reinforcement. The values of thermal stresses σ_{xx}, σ_{yy} and the displacement u are evidently larger with reinforcement when compared with those in the absence of reinforcement. It is clear from this investigation that the surface waves in the fibre-reinforced medium are affected by the reinforcement parameters.

Figures 8, 9, 10, 11, 12 and 13 depicts six representative curves for the distribution of the temperature θ, the displacements u and v and the distributions of stresses σ_{xx}, σ_{yy}, and σ_{xy} both in the absence and presence of rotation Ω. We notice that the results for the temperature, the displacement and stress distribution with the rotation Ω of the medium included in the equation of motion are distinctly different from those without the rotation, $\Omega = 0$, i.e., the thermoelastic wave is affected by rotation. It has also been observed that, at constant $v = 0.5$, the rotation Ω of the medium decreases the values of u, θ and σ_{xy} and increases the values of thermal stresses σ_{xx}, σ_{yy} and the displacement v. Figure 8 shows that the rotation has negligibly small effects on temperature θ although they provide a significant advantage in numerical computations. The study may be useful in construction and design of gyroscopes and rotation sensors. The thermal stresses have significantly large values in the case of a rotating thermoelastic plate as compared with a non-rotating one.

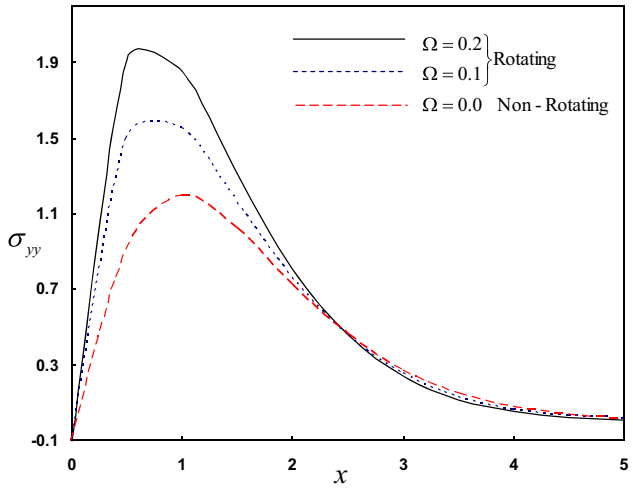

Figure 12. The stress σ_{yy} distribution in the case of material with phase lags in the absence and presence of rotating.

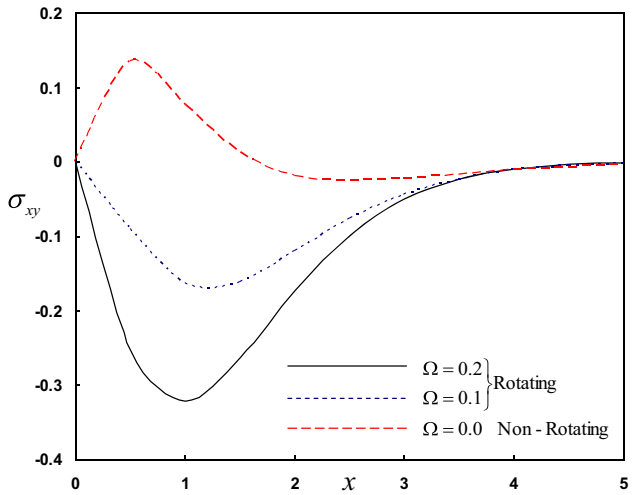

Figure 13. The stress σ_{xy} distribution in the case of material with phase lags in the absence and presence of rotating.

8. Conclusion

Analytical solutions based on the normal mode analysis for the themoelastic problem in solids have been developed and utilized. A linear opening mode-I crack has been investigated and studied for a copper solid. Temperature, radial and axial distributions are estimated at different distances from the crack edge. The stress distributions and the temperature are evaluated as functions of the distance from the crack edge. The cases of reinforcement and the presence and absence of rotation have been addressed. Analytical solutions based upon normal mode analysis for thermoelasticity with fractional order in solids have been developed and utilized. From the present analysis we arrive at the following conclusions:

1. The method that is used in the present article is applicable to a wide range of problems in thermodynamics and thermoelasticity.
2. It has also been found that the physical quantities are affected both by rotation as well as by the phase lags parameters. Therefore, the presence of phase lags parameter and rotation in the current model is of significance.
3. The values of all the physical quantities converge to zero with an increase in distance x and all functions are continuous.
4. The fibre-reinforcement has an important role on the distributions of the field quantities.
5. For figures 2–7, we take the reinforcement to be zero in the program and compare with and without reinforcement.
6. The theories of CTE and generalized thermoelasticity can be obtained as limited cases.
7. Deformation of a body depends on the nature of the forces applied as well as the type of boundary conditions.
8. Crack dimensions are significant to elucidate the mechanical structure of the solid. Cracks are stationary, and external stress is required to propagate such cracks.
9. Conclusions about the new theory of thermoelasticity have been obtained based on numerical results and graphs. The results provide a motivation to investigate conducting materials as a new class of applicable materials.
10. The effect of the phase lag of the heat flux τ_q and the phase lag of gradient of temperature τ_θ is significantly clear on the real parts of the displacements, temperature and thermal stresses.
11. The DPL model is close to LS model. This is in agreement with Hetnarski and Ignaczak [46] (the DPL model is an extension of the LS model).

References

[1] Biot M 1956 Thermoelasticity and irreversible thermo-dynamics. *J. Appl. Phys.* 27: 249–253
[2] Nowacki W 1975 *Dynamic problems of thermoelasticity*. Leyden, The Netherlands: Noordhoff
[3] Nowacki W 1986 *Thermoelasticity*, 2nd ed. Oxford: Pergamon Press
[4] Lord H W and Shulman Y 1967 A generalized dynamical theory of thermoelasticity. *J. Mech. Phys. Solids* 15: 299–309
[5] Green A E and Lindsay K A 1972 Thermoelasticity. *J. Elast.* 2: 1–7
[6] Green A E and Naghdi P M 1993 Thermoelasticity without energy dissipation. *J. Elast.* 31: 189–209
[7] Ignaczak J and Ostoja-Starzewski M 2010 *Thermoelasticity with finite wave speeds*. New York: Oxford University Press, p. 413
[8] Tzou D Y 1995 A unified approach for heat conduction from macro- to micro- scales. *J. Heat Transfer* 117: 8–16

[9] Tzou D Y 1995 Experimental support for the lagging behavior in heat propagation. *J. Thermophys. Heat Transfer* 9: 686–693

[10] Tzou D Y 1996 *Macro- to microscale heat transfer: the lagging behavior*. Washington, DC: Taylor and Francis

[11] Belfield A J, Rogers T G and Spencer A J M 1983 Stress in elastic plates reinforced by fibre lying in concentric circles. *J. Mech. Phys. Solids* 31: 25–54

[12] Verma P D S and Rana O H 1983 Rotation of a circular cylindrical tube reinforced by fibers lying along helices. *Mech. Mater.* 2: 353–359

[13] Sengupta P R and Nath S 2001 Surface waves in fibre-reinforced anisotropic elastic media. *Sadhana* 26: 363–370

[14] Hashin Z and Rosen W B 1964 The elastic moduli of fibre-reinforced materials. *J. Appl. Mech.* 31: 223–232

[15] Singh B and Singh S J 2004 Reflection of planes waves at the free surface of a fibre-reinforced elastic half-space. *Sadhana* 29 : 249–257

[16] Singh B 2007 Wave propagation in an incompressible transversely isotropic fibre-reinforced elastic media. *Arch. Appl. Mech.* 77: 253–258

[17] Singh B 2007 Effect of anisotropy on reflection coefficients of plane waves in fibre-reinforced thermoelastic solid. *Int. J. Mech. Solids* 2: 39–49

[18] Kumar R and Gupta R 2009 Dynamic deformation in fibre-reinforced anisotropic generalized thermoelastic solid under acoustic fluid layer. *Multidisc. Model. Mater. Struct.* 5(3): 283–288

[19] Ailawalia P and Budhiraja S 2011 Fibre-reinforced generalized thermoelastic medium under hydrostatic initial stress. *Engineering* 3: 622–631

[20] Abbas I A and Abd-Alla A N 2011 Effect of initial stress on a fiber-reinforced anisotropic thermoelastic thick plate. *Int. J. Thermophys.* 32(5): 1098–1110

[21] Allam M N, Elsibai K A and Abouelregal A E 2009 Electromagneto-thermoelastic problem in a thick plate using Green and Naghdi theory. *Int. J. Eng. Sci.* 47: 680–690

[22] Cheng J C and Zhang S Y 2000 Normal mode expansion method for laser generated ultrasonic Lamb waves in orthotropic thin plates. *Appl. Phys. B* 70: 57–63

[23] Paria G 1962 On magneto-thermo-elastic plane waves. *Math. Proc. Cambridge Philos. Soc.* 58: 527–531

[24] Wilson A J 1963 The propagation of magneto-thermoelastic plane waves. *Math. Proc. Cambridge Philos. Soc.* 59: 438–488

[25] Schoenberg M and Censor D 1973 Elastic waves in rotating media. *Q. J. Mech. Appl. Math.* 31: 115–125

[26] Puri P 1976 Plane thermoelastic waves in rotating medium. *Bull. Acad. Polon. Sci. Ser. Sci. Tech.* 24: 137–144

[27] Roychoudhury S K and Debnath L 1984 Magnetoelastic plane waves in infinite rotating media. *Trans. ASME J. Appl. Mech.* 106: 283–287

[28] Roychoudhury S K 1985 Effect of rotation and relaxation times on plane waves in generalized thermoelasticity. *J. Elast.* **15**, 59–68

[29] Chandrasekharaiah D S and Srikantiah K R 1984 Thermoelastic plane waves in a rotating solid. *Acta Mech.* 50: 211–219

[30] Chandrasekharaiah D S 1986 Temperature-rate dependent electromagneto-thermoelastic plane waves in a rotating solid. *Int. J. Eng. Sci.* 24(7): 1173–1184

[31] Abo-Dahab S M 2012 Influence of magneto-thermo-viscoelasticity in an unbounded body with a spherical cavity subjected to harmonically varying temperature without energy dissipation. *Meccanica* 47(3): 613–620

[32] Abouelregal A E and Abo-Dahab S M 2012 Dual phase lag model on magneto-thermoelasticity infinite nonhomogeneous solid having a spherical cavity. *J. Therm. Stresses* 35(9): 820–841

[33] Mahmoud S R 2013 On problem of shear waves in magneto-elastic half-space of initially stressed non-homogeneous anisotropic material under influence of the rotation. *Int. J. Mech. Sci.* 77: 269–276

[34] Abd-Alla A M, Nofal T A, Abo-Dahab S M and Al-Mullise A 2013 Surface waves propagation in fibre-reinforced anisotropic elastic media subjected to gravity field. *Int. J. Phys. Sci.* 8(14): 574–584

[35] Abd-Alla A M, Abo-Dahab S M and Al-Mullise A 2013 Effects of rotation and gravity field on surface waves in a fibre-reinforced thermoelastic media under four theories. *J. Appl. Math.* 2013: 20

[36] Abouelregal A E and Abo-Dahab S M 2014 Dual-phase-lag diffusion model for Thomson's phenomenon on elctromagneto-thermoelastic an infinitely long solid cylinder. *J. Comput. Theoret. Nanosci.* 11(4): 1031–1039

[37] Abd-Alla A M and Abo-Dahab S M 2015 Effect of initial stress, rotation and gravity on propagation of the surface waves in fibre-reinforced anisotropic solid elastic media. *J. Comput. Theoret. Nanosci.* 12(2): 305–315

[38] Abo-Dahab S M, Abd-Alla A M and Aftab Khan 2015 Magnetism and rotation effect on surface waves in fibre-reinforced anisotropic general viscoelastic media of higher order. *J. Mech. Sci. Tech.* 29(8): 3381–3394

[39] Abo-Dahab S M and Lotfy Kh 2015 Generalized magneto-thermoelasticity with fractional derivative heat transfer for a rotation of a fibre-reinforced thermoelastic. *J. Comput. Theoret. Nanosci.* 12(8): 1869–1881

[40] Abd-Alla A M, Khan A and Abo-Dahab S M 2015 Rotational effect on Rayleigh, Love and Stoneley waves in fibre-reinforced anisotropic general viscoelastic media of higher and fraction orders with voids. *J. Mech. Sci. Technol.* 29(10): 4289–4297

[41] Khan A, Abo-Dahab S M and Abd-Alla A M 2015 Gravitational effect on surface waves in a homogeneous fibre-reinforced anisotropic general viscoelastic media of higher integer and fractional order with voids. *Int. J. Phys. Sci.* 10(24): 604–613

[42] Abd-Alla A M, Othman M I A and Abo-Dahab S M 2016 Reflection of plane waves from electro-magneto-thermoelastic half-space with a Dual-Phase-Lag model. *Comput. Mater. Continua* 51(2): 63–79

[43] Elsagheer M and Abo-Dahab S M 2016 Reflection of thermoelastic waves from insulated boundary fibre-reinforced half-space under influence of rotation and magnetic field. *Appl. Math. Inform. Sci.* 10(3): 1–11

[44] Abd-Alla A M, Abo-Dahab S M and Khan A 2017 Rotational effect on thermoelastic Stoneley, Love and Rayleigh waves in fibre-reinforced anisotropic general viscoelastic media of higher order. *Struc. Eng. Mech. Int. J.* 61(2): 221–230

[45] Lotfy Kh 2012 Mode-I crack in a two-dimensional fibre-reinforced generalized thermoelastic problem. *Chin. Phys. B* 21(1): 014209

[46] Hetnarski R B and Ignaczak J 1999 Generalized thermoelasticity. *J. Therm. Stresses* 22: 451–476